Mode Assignment of Sulfur α-S_8 by Polarized Raman and FTIR Studies at Low Temperatures

M. Becucci,* R. Bini, and E. Castellucci

European Laboratory for Non-Linear Spectroscopy, Largo Enrico Fermi 2, 50125 Florence, Italy

B. Eckert and H. J. Jodl

Fachbereich Physik, Universität Kaiserslautern, E.Schrödinger Strasse, 67653 Kaiserslautern, Germany

Received: October 2, 1996; In Final Form: December 16, 1996[⊗]

We have measured frequencies of all internal and external modes in natural and ^{32}S isotopically pure oriented orthorhombic single sulfur crystals using high-resolution Raman and FTIR spectroscopy. Polarized spectra at low temperatures deliver mode frequencies and allow mode assignment to vibrational, librational, and translational character. Experimental data, such as temperature dependent frequencies at constant volume, are analyzed in terms of anharmonic processes. In addition, frequency shifts at the lowest temperature due to isotopic impurities are qualitatively explained by a relative mass defect.

1. Introduction

The molecular crystal of sulfur α-S_8 has been the subject of several previous spectroscopic studies from theoretical and experimental points of view. The available information, however, is not accurate; i.e., most authors report mode wavenumbers differing by more than ±2 cm^{-1} and their assignment is not consistent. In addition, neither internal nor external potentials are adequate to model internal or external frequencies.

S_8 molecular sulfur crystallizes in an orthorhomic phase (space group F_{ddd} (D_{2h}^{24})), with four S_8 molecules (free molecule symmetry D_{4d}) per primitive unit cell located on sites having C_2 symmetry.[1] In Table 1 we show the correlation diagram for the 72 internal and 24 external crystal components with the relative infrared (IR) and Raman (R) activities.

Vibrational spectroscopic data were collected by Raman scattering from natural sulfur (S_{nat}) crystals or powder at 300,[2,5,6] 100,[3] 77,[11] 40,[14] 30,[7] and 16 K[15] and by IR absorption on S_{nat} crystals at 100,[4] 30,[7] 10,[16,17] and 4 K.[10] In addition, polarized spectra from oriented single crystals were measured both by Raman[5,6,7,15] and IR techniques.[7,16,17] Isotope-free α-$^{32}S_8$-oriented single crystals were investigated only recently by polarized Raman[15] and polarized FTIR techniques.[16,17] According to our knowledge, there is only one neutron study by Rinaldi et al.[9] Theoretical calculations were performed to reproduce external modes by a shell model for molecular crystals[8] to calculate Raman intensities in an oriented single crystal of α-S_8[12] and to model internal as well as external modes by a nonrigid molecular model.[13]

By comparison of all these spectroscopic results, the above-mentioned inconsistencies in mode characterization arise from experimental limitations such as not fully resolved crystal field splitting due to too high temperatures, spectra complicated by isotope components in spectra of S_{nat}, overlap of different polarization components due to ill-defined light-scattering geometry with respect to sample geometry.

Our aim is to give a detailed account of the vibrational spectroscopic properties of the S_8 crystal based on careful sample preparation, i.e., use of oriented single crystals of S_{nat} with isotopes and pure ^{32}S, low-temperature experiments (T < 20 K), and finally modern instruments. These efforts were made to provide accurate frequencies and an almost unambigous assignment of internal as well as external modes. This complete set of data may then act as an input for further theoretical considerations to model an internal and an external potential for sulfur of better quality than up to now.

TABLE 1: Correlation Diagram for Internal and External Vibrations of Orthorombic Sulfur S_8

Vibrations		Molecular symmetry	Site symmetry	Factor group symmetry
internal 11	external 6	D_{4d}	C_2	D_{2h}
ν_1, ν_2		a_1 (R)		a_g (R)
	L_z	a_2 (-)		b_{1g} (R)
ν_3		b_1 (-)	a	b_{2g} (R)
ν_4	T_z	b_2 (IR)		b_{3g} (R)
ν_5, ν_6	T_x, T_y	e_1 (IR)	b	a_u (-)
ν_7, ν_8, ν_9		e_2 (R)		b_{1u}(IR)
ν_{10}, ν_{11}	L_x, L_y	e_3 (R)		b_{2u} (IR)
				b_{3u} (IR)

2. Experimental Section

Single crystals of natural and isotopically pure (99.95% of ^{32}S) sulfur were grown from $CHCl_3$ solution after several crystallizations from the same solvent. These samples were cut along the crystal axes in the shape of cubes, with sides of about 2 mm, for Raman studies or were cut in the form of thin slabs of about 4−5 mm diameter polished to a thickness ranging from 350 to 450 μm for infrared studies. The slab was always oriented with the *c* axis lying in the plane because it turned out that in the crystal growing this was the preferred orientation. The crystal axes in the crystals were determined by use of X-rays.

The single crystals were placed in a copper holder immersed in a liquid He cryostat during Raman measurements ($T \approx 5$ K) or mounted in a variable temperature closed cycle He cryostat ($T \approx 8$ and 16 K, according to two systems with different cooling power) in the infrared experiments. These final temperatures did not affect the frequencies (below 20 K the curve frequency versus temperature $\omega(T)$ is flat; see Figure 3) but did affect bandwidths and the deconvolution of crystal field

* To whom correspondence should be addressed. E-mail: becucci@lens.unifi.it.

[⊗] Abstract published in *Advance ACS Abstracts,* February 1, 1997.

S1089-5647(96)03029-5 CCC: $14.00

components in spectra. The temperature was measured by calibrated Si diodes with an error of ±0.1 K and checked in Raman experiments by the intensity ratio between Stokes and anti-Stokes components of lattice modes.

The infrared spectra were measured using a Bruker IFS 120 high-resolution FTIR spectrometer equipped with a He-cooled bolometer. Wavenumbers were measured with an error of ±0.01 cm^{-1} thanks to the calibration of the Fourier spectrometer with a He−Ne laser. The resolution was better than 0.05 cm^{-1}. The Raman spectrometer consisted of a double monochromator (Jobin Yvon Model U 1000) with the wavenumber calibrated against atomic lines to ±0.1 cm^{-1} and with a maximum resolution of 0.2 cm^{-1}. By the insertion of a Fabry−Perot interferometer (Burleigh 110) in the optical path, the resolution rose to 0.005 cm^{-1}, revealing complex structures unresolved by the limited instrumental function of the monochromator.

Polarized Raman experiments were performed on the oriented single crystals in all the polarization geometries so that all the Raman active factor group components (a_g, b_{1g}, b_{2g}, and b_{3g}) were identified. Polarized infrared spectra were able to separate, owing to sample growing, only the b_{1u} (parallel to the *c* axis) and $b_{2u} + b_{3u}$ components (perpendicular to *c* axis). The b_{2u} and b_{3u} components were later identified on samples obtained by reducing large natural S_8 crystals.

3. Results and Discussion

In the primitive unit cell there are four S_8 molecules. Therefore, each nondegenerate mode ($\omega_1 - \omega_4$; T_z, L_z) splits into four factor group components while degenerate modes ($\omega_5 - \omega_{11}$; T_x, T_y, L_x, L_y) give eight different components. From the correlation diagram (see Table 1) the symmetry and the activity of the crystal components result. The survey spectra (Figure 1a shows Raman scattering; Figure 1b shows IR absorption) present the phonon and internal regions. The relative intensities mirror clearly the different Raman and IR activities of the modes of the free S_8 ring (see Table 1). As an example, we display in Figure 2 the well-resolved and unambigously assigned crystal field components of the internal ω_8 mode. Table 2 contains the frequencies of all components of internal ($\omega_1 - \omega_{11}$) and external (libration L, translation T) modes. Remarkable is that all frequency values are always slightly smaller in the S_{nat} than in the ^{32}S crystal (see Table 2). The error in frequency arises from the resolution of the spectrometers and the uncertainty of determining frequencies from band maxima (band shape analysis). The error in the wavenumber is therefore estimated to be <0.05 cm^{-1}.

Assignment of External Vibrations. By comparison of our polarized spectra (at $T = 4-20$ K) with the ones from literature (at 30 and 300 K),[5−7] the agreement in assigning symmetry components (a_g, b_{1g}, b_{2g}, b_{3g}, b_{1u}, b_{2u}, b_{3u}) is good. In comparison to literature results, some of these frequencies differ by ±5 cm^{-1}, but most of the frequencies determined by different authors coincide, especially if one considers a frequency shift to smaller energies by about 1.5−2 cm^{-1} on raising the temperature by $\Delta T \approx 250$ K. We carefully determined this temperature dependence of frequencies. There also exists now an agreement about the fact that modes with mostly translational character T are located at higher frequencies with respect to modes with mostly librational character L.

Our Assignment Procedure. Owing to group theory (Table 1) the libration around the *z* axis (L_z) is inactive. Therefore, we assigned this libration to the lowest lying doublets, weak in Raman as well as in IR spectra, having the following wavenumbers (cm^{-1}): 31.5 (b_{2g}), 32.6 (b_{3g}), 33.83 (b_{3u}), and 35.80 (b_{2u}). The libration $L_{x,y}$ are supposed to be the only Raman active components. Therefore, we assigned the strongest Raman features to these modes: 54.5 cm^{-1} (a_g), 41.2 cm^{-1} (b_{1g}), 53.98 cm^{-1} (b_{2g}), and 45.8 cm^{-1} (b_{3g}); see Figure 1a. Then we looked for the strongest IR components with high frequencies (see Figure 1b) and assigned them according to group theory as a translation T_z with two components at 62.46 cm^{-1} (b_{3u}) and 76.46 cm^{-1} (b_{2u}). We expect the equivalent Raman active components to be weak in that spectral range, and they are 69.5 cm^{-1} (b_{3g}) and 77.8 cm^{-1} (b_{2g}). However, since the L_x, L_y components should be weak in the IR spectra, we assigned those features to 41.75 cm^{-1} (b_{1u}), 53.16 cm^{-1} (b_{3u}), and 54.51 cm^{-1} (b_{2u}). At the end, missing were the IR active T_x,T_y excitations with weak components in the Raman spectra (see Figure 1a) at 58.4 cm^{-1} (a_g), 61.3 cm^{-1} (b_{1g}), 64.9 cm^{-1} (b_{2g}), and 61.3 cm^{-1} (b_{3g}). From neutron spectra[9] only a little is known about some frequencies of the acoustic modes (b_{1u}, b_{2u}, b_{3u} with translational character).

Our tentative assignment was based on the correlation among Raman and IR intensities and the activity expected by group theory. This is only an approximated procedure because in the site symmetry the distinction between librational and translational motions is lost (see Table 1). As a result, all the phonons will have mixed character. A normal coordinate analysis was performed by D. Dows (private communication) using an atom−atom potential with charge transfer. These results show that some modes mantain pure character i.e., translation or libration around one axis. A normal mode analysis based on better potentials, including quadrupole and anisotropic terms, should be tested to specify their librational/translational characted more precisely.

Even if the internal modes ω_9 are close to the T_z mode, we could clearly resolve both features. There are two arguments. (1) At about 75 cm^{-1} the lattice phonons and the vibrons (crystal field components of ω_9) are close together, if not overlapping. Theoretical considerations predict some mixing of the eigenvector components of these two modes,[13] which is experimentally proven by their temperature and pressure dependence. The temperature dependence is very similar to that of the lattice phonons below 75 cm^{-1}.[19] The pressure dependence of the modes between 75 and 100 cm^{-1} is intermediate (Grüneisen parameter $\gamma \cong 0.6-0.7$) between the lattice phonons ($\gamma > 0.5$) and the remaining vibrons ($\gamma < 0.5$).[18] (2) Since the effect of isotopic substitution is larger for internal than for external mode frequencies (see later), this would help to resolve both regions because the observed frequency shifts are—with respect to error and resolution in Raman and IR spectra—generally larger in the case of ω_9 components (0.2−0.5 cm^{-1}) than in the case of lattice modes (<0.2 cm^{-1}). Moreover, the two lowest IR active ω_9 components show an isotopic splitting not expected for lattice modes (see later).

Finally, we are able to solve the assignment problem of the two lowest lying Raman components measured around 30 cm^{-1}. At $T = 300$ K these modes were assigned at 28 cm^{-1} (b_{3g}) and 29 cm^{-1} (b_{2g}),[5] and 26.5 cm^{-1} (b_{3g}) and 29 cm^{-1} (b_{2g}).[6] At 30 K an unresolvable feature was observed at 30 cm^{-1},[7] whereas at 4 K we clearly resolved both components (Figure 1a) and assigned them with reversed symmetry due to polarized spectra: 31.5 cm^{-1} (b_{2g}) and 32.6 cm^{-1} (b_{3g}). The straightforward explanation is a crossing of two modes with different symmetries on lowering the temperature (about 50 K [15]). This interpretation is confirmed by a similar crossing of these specific modes with rising pressures at room temperatures (about 1 GPa [18]). Each component has a different temperature or pressure coefficient of mode energies.

Assignment of Internal Vibrations. The following internal modes are now accurately measured, well resolved in crystal field components and therefore correctly assigned, in agreement

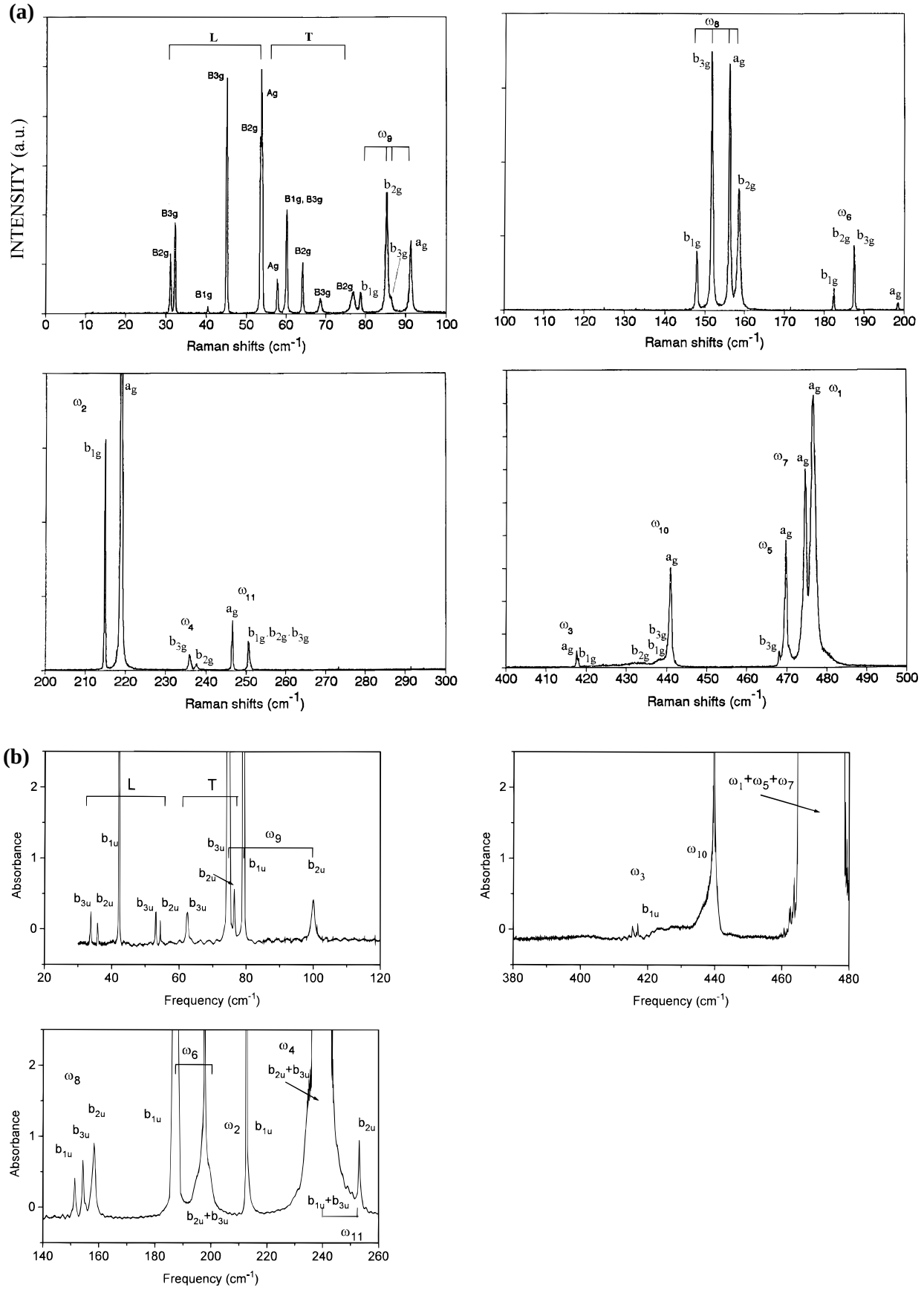

Figure 1. Survey spectra of α-S_8: (a) Raman scattering of α-$^{32}S_8$ at 15 K and (b) IR absorption of S_{nat} at 8 K with mode assignment of crystal field components for internal and external excitations. L and T stand for librational and translational external modes, respectively.

with literature results, e.g., ω_9 (torsion at 86 cm^{-1} in the free ring), ω_8 (bending at 152 cm^{-1}), ω_6 (b at 180 cm^{-1}), ω_2 (b at 218 cm^{-1}).[7]

The ω_4 (b at 243 cm^{-1}) is off scale in IR absorption but the expected Raman components are clearly resolved and assigned. For the ω_{11} (b at 248 cm^{-1}) mode only two out of four Raman components could be well determined (a_g, b_{2g}, whereas b_{1g} and b_{3g} are very weak[12] and possibly degenerate with b_{2g}), whereas in IR absorption this Raman active mode reveals the b_{1u} and b_{2u} components, but the b_{3u} component is lying in the manifold

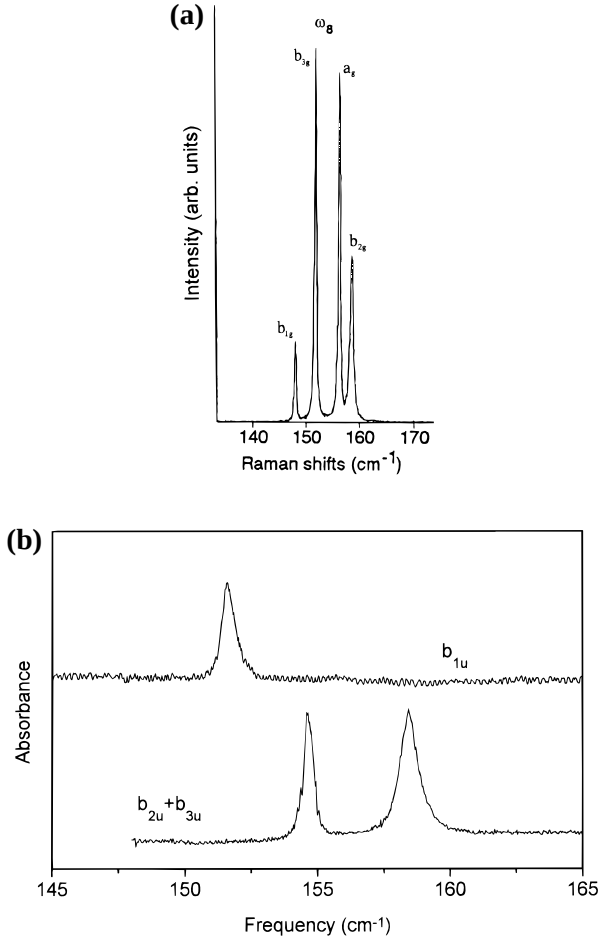

Figure 2. ω_8 region: (a) polarized Raman spectra of ^{32}S oriented single crystals at $T \approx 15$ K; (b) polarized IR absorption of ^{32}S oriented single crystals at $T \approx 17$ K .

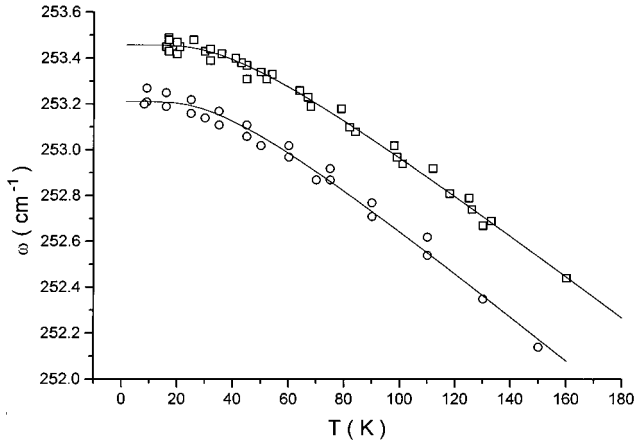

Figure 3. Temperature dependence of one internal mode (b_{2u} component of ω_{11}): (○) natural crystal; (□) pure ^{32}S crystal. Solid lines are calculated according to eq 3 with $B = 1.0$ cm^{-1} and $\bar{\omega} = 70-80$ cm^{-1} for both cases.

of ω_4. The ω_3 (stretch at 417 cm^{-1}) possesses two well-resolved Raman lines; the IR absorption is obscured by isotope lines. Using isotope pure ^{32}S crystals, we found only one component as expected.[16] The ω_{10} (stretch at 437 cm^{-1}) shows all four Raman components, a few broadened. The IR spectrum is very weak in that region—next to the strong absorption of ω_5—and reveals the b_{2u} and b_{3u} components, whereas the b_{1u} is missing. The ω_5 (stretch at 471 cm^{-1})—being an IR active mode in the isolated molecule—is off scale, while the Raman spectrum contains all four expected components. The ω_1 (stretch at 475 cm^{-1}) and ω_7 (stretch at 475 cm^{-1})—as Raman active modes

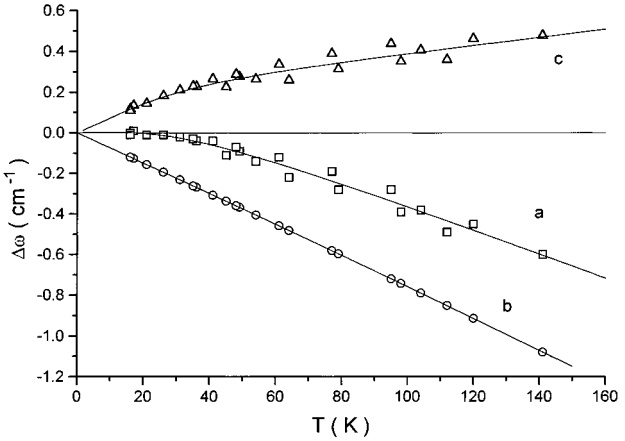

Figure 4. Relative wavenumber shift of the external mode at 34 cm^{-1} of pure ^{32}S crystal as a function of temperature: (a) fit of the experimental data (□); (b) volume contribution to the shift; (c) difference between (a) and (b).

in the isolated molecule—give rise to a strong broad Raman spectrum in which we could only identify the a_g component. This is in accordance with the calculated Raman intensities,[12] which are, for the a_g components of all three stretching modes, much larger than for the other components. The IR spectrum of these two modes is mainly influenced by the very strong absorption due to the ω_5 mode, and only the b_{1u} component of ω_7 is well resolved.

The overall intensity pattern of the internal Raman active modes (Figure 1a) is nicely modeled by ref 12, besides the ω_{10} and $\omega_1/\omega_5/\omega_7$ regions.

Finally, the analysis of the polarized Raman spectra contained no problem with respect to intensities, bandwidth, etc. However, the analysis of the IR absorption spectra caused some problems because in the two regions of ω_4/ω_{11} and $\omega_1/\omega_5/\omega_7$, the modes were off scale (Figure 1b). We tried to decrease sample thickness (starting with ~300μm), but we would need at least 1 order of magnitude thinner slabs; thinned samples (~100μm) either break mechanically or crack during sample cooling.

Temperature Dependence and Anharmonicity. As pointed out in the Introduction, Raman and IR spectra were investigated up to now only at a few temperatures. We measured and analyzed Raman spectra between 5 and 250 K.[18,19] Here, we would like to present our complementary data collected by IR absorption between 10 and 140 K and will discuss one internal (Figure 3) and one external mode (Figure 4) representatively.

In general mode frequencies ω and the bandwidth Γ of a crystal vibration depend on the temperature T in a rather complex but similar way. These anharmonic corrections to mode frequency ω and bandwidth Γ can be separated into an explicit dependence on T because of phonon−phonon interaction and an implicit dependence on T due to volume expansion:

$$\omega \text{ or } \Gamma \approx f(T, V(T)) \qquad (1)$$

The whole complex $\Gamma(T)$ is published recently elsewhere[17] and interpreted in terms of relaxation processes.

The experimental frequency shift $\omega(T)$ for the internal mode $\omega_{11} = 253$ cm^{-1} (b_{2u} component) and the relative frequency shift $\Delta\omega(T) = \omega(T) - \omega(T = 0\text{ K})$ for the external mode at 34 cm^{-1} ($L_z - b_{3u}$ component) in the pure ^{32}S and S_{nat} crystals are plotted in Figures 3 and 4. These shifts cannot be used directly for a discussion of the relaxation processes, since they include the contribution due to thermal expansion of the crystal, which gives rise to a decrease of the vibrational frequency as the temperature increases. The experimental shifts at constant pressure $[\Delta\omega(T)]_p$ and the theoretical anharmonic shifts calcu-

TABLE 2: Frequencies (cm^{-1}) of Internal and External Modes of α-S_8 Crystals[a]

		S_{nat}	^{32}S			S_{nat}	^{32}S
ν_1	a_g	476.8	477.5		b_{1g}	79.2	79.6
	b_{1g}	?	~480		b_{2g}	85.8	86.3
	a_u				b_{3g}	shoulder at 87	shoulder at 87
	b_{1u}	478.1	478.0		a_u		
ν_2	a_g	218.6	219.1		b_{1u}	78.47 and 79.62 i	79.10
	b_{1g}	214.4	215.1		b_{2u}	99.75	99.96
	a_u				b_{3u}	74.12 and 74.62 i	74.43
	b_{1u}	212.4 and 213.7 i	213.3	ν_{10}	a_g	440.3	441.5
ν_3	a_g	416.2	417.6		b_{1g}	438.2	438.5
	b_{1g}	417.8	418.0		b_{2g}	~433	433.6
	a_u				b_{3g}	~440	440.8
	b_{1u}	417.09 (multiplet) i	416.82		a_u		
ν_4	b_{2g}	238?	236.6		b_{1u}	440.2	439.4 shoulder
	b_{3g}	236?	236.2		b_{2u}	440.2	439.8
	b_{2u}		238?		b_{3u}	437	437.2 shoulder
	b_{3u}		241	ν_{11}	a_g	246.8	246.9
ν_5	a_g	470.0	470.5		b_{1g}	251.4	250.8
	b_{1g}	(465.6 i)	?		b_{2g}	251.4	250.8
	b_{2g}	(464.0 i)	?		b_{3g}	251.4	250.8
	b_{3g}	467.7	469.1		a_u		
	a_u				b_{1u}		~241
	b_{1u}	472.3	472.4		b_{2u}	253.21	253.46
	b_{2u}	469.5	469.7		b_{3u}		~240
	b_{3u}	473.8	474.8			Librations	
ν_6	a_g	198	198.9	L_z	b_{2g}	31.4	31.5
	b_{1g}	183	183.1		b_{3g}	32.6	32.6
	b_{2g}	187.6	188.4		b_{2u}	35.74	35.80
	b_{3g}	187.6	188.4		b_{3u}	33.76	33.83
	a_u			L_yL_x	a_g	54.4	54.5
	b_{1u}		186.6		b_{1g}	40.8	41.2
	b_{2u}		196.7		b_{2g}	54.4	53.98
	b_{3u}		199.2		b_{3g}	45.6	45.8
ν_7	a_g	475	475.0		a_u		
	b_{1g}	?			b_{1u}	41.75	41.75
	b_{2g}	?			b_{2u}	54.48	54.51
	b_{3g}	?			b_{3u}	53.13	53.16
	a_u					Translations	
	b_{1u}	465.5	467.2	T_z	b_{2g}	77.2	77.8
	b_{2u}	471.2	471.3		b_{3g}	69.2	69.5
	b_{3u}	467.4	468.6		b_{2u}	76.37	76.46
ν_8	a_g	156.2	157.2		b_{3u}	62.32	62.46
	b_{1g}	148.4	149.0	T_xT_y	a_g	58.4	58.4
	b_{2g}	158.6	159.4		b_{1g}	60.0	61.3
	b_{3g}	152	152.6		b_{2g}	64.6	64.9
	a_u				b_{3g}	60.8	61.3
	b_{1u}	151.4	151.6		a_u		
	b_{2u}	158.2	158.4		b_{1u}		
	b_{3u}	154.5	154.7		b_{2u}		
ν_9	a_g	91.6	92.0		b_{3u}		

[a] i indicates that isotope peaks are also observed.

lated at constant volume $[\Delta\omega(T)]_V$ are related by the following equation:[20]

$$[\Delta\omega(T)]_p = [\Delta\omega(T)]_V + \omega(0)\{\exp[-\gamma \ln(V(T)/V(0))] - 1\} \quad (2)$$

where γ is the single vibron Grüneisen parameter given by $\gamma = -\partial \ln \omega(T)/\partial \ln V(T)$. In this equation the first term is the above-mentioned explicit term and the second one the implicit term.

These corrected frequency shifts at constant volume can now be fitted by the following equation and interpreted according to the well-known relaxation processes containing contributions due to scattering, decay, and dephasing processes (for basic information, see, for example, ref 21).

$$[\Delta\omega(T)]_V = -Bn(\bar{\omega},T) \quad (3)$$

where B is a coupling constant, which relates directly to derivatives of the interaction potential, and $n(\bar{\omega},T)$ is the occupation number of phonons and ϖ an average bath phonon.

The inspection of all experimental data, e.g., Figures 3 and 4, shows that mode frequencies at $T = 0$ K for the pure ^{32}S crystal in comparison to the S_{nat} crystal are slightly larger (isotopic effect; see later), the temperature dependence is similar in the ^{32}S and S_{nat} crystals, and the slope is typically $\Delta\omega/\Delta T \approx -10^{-3}$ cm $^{-1}$ K^{-1} in the classical limit (large T).

Next we will separate the two anharmonic contributions (eq 2) by analyzing the temperature dependence of the external mode at 34 cm $^{-1}$ (Figure 4). A similar consideration for an internal mode such as ω_{11} (Figure 3) is already published for the ω_3 at 417 cm^{-1}.[16] We have calculated the second term in (2) using a mode Grüneisen parameter γ from ref 18 and a volume expansion $V(T)$ from ref 22. Subtracting this volume contribution to the shift (line b in Figure 4) from the experimental data (line a in Figure 4), we obtain the wanted anharmonic shift at constant volume (line c in Figure 4), which is positive and increases linearly with temperature and whose slope changes significantly at about 30 K. The relaxation of this mode was interpreted according to cubic down (34 cm^{-1} → 17 cm^{-1} + 17 cm^{-1}) and up (34 cm^{-1} + 34 cm^{-1} → 68

cm^{-1}) processes on the basis of our bandwidth analysis.[17] Below 20 K, owing to the low population of the thermal bath, only the down processes are active. As the temperature exceeds 25 K, the up processes become rapidly dominant. Taking advantage of these results, the c curve of Figure 4 can be explained on the basis of an opposite sign of down and up processes contributing to the frequency shift; i.e., the down processes contribution with a positive sign to the shift is dominated at $T > 30$ K by the up processes contribution with a negative sign. This interpretation of $[\Delta\omega(T)]_V$ is consistent with our interpretation of the temperature dependence of the bandwidth Γ (mode at 34 cm^{-1}) (see Figure 2 of ref 17). Both experimental values must be interpreted similarly, since—owing to theory—both values form the anharmonic correction to mode energies: $\Delta\omega_{anharm} = \Delta\omega_{harm} + \Gamma$.

Some Critical Comments to Figure 4. Since there exist no high-pressure IR data on sulfur—as a first guess—our Raman data at high pressure[18] were used to determine the mode Grüneisen parameter for this IR phonon at 34 cm^{-1}. If we consider all Raman active phonons below 60 cm^{-1}, we find an average value γ of 2.5, which we used above. The uncertainty in γ is mainly governed by the different compressibility values in the literature. In addition, the volume expansion values $V(T)$ are not consistent in the literature. Two different sets of $V(T)$ exist. Owing to technical arguments, we prefer the data by Coppens.[22]

Effect of Isotopic Impurities. Natural sulfur has the following isotopic composition: 95.02% of ^{32}S, 4.22% of ^{34}S, and 0.76% of ^{33}S isotopes. Accordingly, we expect that the most abundant molecular species represented in the crystal are 66.4% of molecules $^{32}S_8$, 23.6% of molecules $^{34}S_1{}^{32}S_7$, 4.3% of molecules $^{33}S_1{}^{32}S_7$, and 3.7% of molecules $^{34}S_2{}^{32}S_6$. Therefore, only 6% of the S_8 rings contain more than one isotopic impurity. So it is sufficient in the following to compare $^{32}S_8$ with $^{34}S_1{}^{32}S_7$ only. The doping by this kind of impurity will cause several effects: additional isotopic bands well separated from the pure one (e.g., ω_3 of sulfur discussed in ref 16); band broadening Γ_{nat} ($T = 0$ K) > Γ_{pure} ($T = 0$ K) as discussed for sulfur in refs 15 and 17; frequency shift $\Delta\omega_{iso} = \omega_{32S}(T = 0\ K) - \omega_{Snat}(T = 0\ K)$.

Qualitatively, these mode energies are shifted to smaller values because an isotopic impurity with slightly larger mass is doped into an S_8 ring. Table 2 contains about 30 internal vibrations delivering an average shift of $\Delta\omega$(vibr.) ≈ 0.6 cm^{-1}. Eight librations generate an average shift of $\Delta\omega$(libr.) ≈ 0.1 cm^{-1}, and seven translations generate $\Delta\omega$(trans.) ≈ 0.3 cm^{-1}. Therefore, the shift is about 3 times larger in the case of internal modes than of external modes.

Looking more quantitatively at these frequency shifts due to isotopic impurities, we cannot recognize an obvious trend such as $\Delta\omega$ as a function of ω or a trend due to symmetry classes of modes (see Table 1). Of course, only a normal coordinate analysis would clarify this mode selective frequency behavior due to isotope impurities, whereas this factor of 3 between internal and external modes is easily understood. In the case of translational and librational motions of a molecule as a whole, what matters is the variation of the total mass and of the inertia moment, respectively. By substitution of one ^{32}S atom in the ring with a ^{34}S isotope, the mass variation $\Delta m/m$ is of 2 atom units over 256. The inertia moments, calculated from the X-ray data of ref 23, are $I_a = I_b = 757.8$ au and $I_c = 1390.2$ au for the $^{32}S_8$ molecule and $I_a = 758$ au, $I_b = 763.4$ au, and $I_c = 1395.6$ au for the $^{34}S_1{}^{32}S_7$ molecule. Therefore, the relative variation $\Delta I/I$ with respect to all axes is of the same order of magnitude as $\Delta m/m$. In the case of an internal vibration, ^{32}S against ^{32}S or ^{34}S against ^{32}S gives a mass variation of 2/64. Consequently, the effect of impurities on internal coordinates is about 4 times larger than the effect on external ones such as the ratio in the experimental data of $\Delta\omega_{iso}$ for internal and external modes.

Conclusion

We summarize available spectroscopic literature (Raman, neutron scattering, and IR absorption) of α-S_8 crystals and point out that there still exist some inconsistencies of mode assignment and scattering of frequencies due to different authors.

Our aim was to repeat polarized Raman and IR spectra using modern apparatus and better samples (isotope-free and natural, oriented single crystals), and we are able to present unambiguously assigned mode frequencies of internal as well as external modes with high quality. In addition, we observed a mode crossing of phonons with different symmetries at very low temperature and identified isotopic components of vibrons. As an example, we studied the anharmonic terms, such as phonon−phonon interaction and the volume term, of a phonon and interpreted the temperature shift of the mode frequency at constant volume in terms of relaxation processes (three-phonon down and up processes mainly). Finally, owing to higher resolution, we detected a frequency shift of all modes at low temperature due to isotopic impurities and explain the size of this shift qualitatively in terms of relative mass defects.

Acknowledgment. This work is supported by the Murst, the C.N.R., and the European Community under Contract GE1* 0046 of the "Large Installation Plan". One of us (H.J.J.) expresses his thanks to NATO (Grant Number 890814).

References and Notes

(1) Warren, B. E.; Burwell, J. T. *J. Chem. Phys.* **1934**, *3*, 6. Abrahams, J. C. *Acta Crystallogr.* **1955**, *8*, 661.

(2) Ward, A. T. *J. Phys. Chem.* **1968**, *72* (2), 745.

(3) Anderson, A.; Loh, Y. T. *Can. J. of Chem.* **1969**, *47*, 879.

(4) Anderson, A.; Wong, L. Y. *Can. J. Chem.* **1969**, *47***,** 2713.

(5) Ozin, G. A. *J. Chem Soc. A* **1969**, 116.

(6) Arthur, J. W.; Mackenzie, G. A. *J. Raman Spectrosc.* **1974**, *2*, 199.

(7) Gautier, G.; Debeau, M. *Spectrochim. Acta* **1974**, *30A*, 1193.

(8) Luty, T.; Pawley, G. S. *Phys. Status Solidi. B* **1975**, *69*, 551.

(9) Rinaldi, R. P.; Pawley, G. S. *J. Phys. C* **1975**, *8*, 599.

(10) Anderson, A.; Boczar, P. G. *Chem. Phys. Lett.* **1976**, *43* (3), 506.

(11) Karonen, A.; Stenman, F. Report Series in Physics HU-P-152; University of Helsinki: Helsinki, 1969.

(12) Domingo, C.; Montero, S. *J. Chem. Phys.* **1981**, *74* (2), 862.

(13) Gramaccioli, C. M.; Filippini, G. *Chem. Phys. Lett.* **1984**, *108* (6), 585. Kurittu, J. V. E. *Phys. Scr.* **1980**, *21*, 200.

(14) Harvey, P. D.; Butler, I. S. *J. Raman Spectrosc.* **1986**, *17*, 329.

(15) Becucci, M.; Castellucci, E.; Foggi, P.; Califano, S.; Dows, D. *J. Chem. Phys.* **1992**, *96* (1), 98.

(16) Eckert, B.; Bini, R.; Jodl, H. J.; Califano, S. *J. Chem. Phys.* **1994**, *100* (2), 912.

(17) Bini, R.; Eckert, B.; Jodl, H. J.; Califano, S. *J. Chem. Phys.* **1997**, *106* (2), 511.

(18) Eckert, B.; Jodl, H. J.; Albert, H. O.; Foggi, P. In *Frontiers of High-Pressure Research*; Hochheimer H. D., Etters, R. D., Eds.; Plenum Press: New York, 1991.

(19) Eckert, B.; Albert, H. O.; Jodl, H. J.; Foggi, P. *J. Phys. Chem.* **1996**, *100*, 8212.

(20) Ouillon, R.; Ranson, P.; Califano, S. *Chem. Phys.* **1984**, *91*, 119.

(21) Califano, S.; Schettino, V.; Neto, N. *Lattice Dynamics of Molecular Crystals*; Springer Series on Lecture Notes in Chemistry 26; Springer: Berlin, 1981.

(22) Coppens, P.; Yang, Y. W.; Blessing, R. H.; Copper, W. F.; Larsen, F. K. *J. Am. Chem. Soc.* **1977**, *99*, 760.

(23) Warren, B. E.; Burwell, J. T. *J. Chem. Phys.* **1934**, *3*, 6. Abrahams, J. C. *Acta Crystallogr.* **1955**, *8*, 661. Rettig, S. J.; Trotter, J. *Acta Crystallogr. C* **1987**, *43*, 2260.